TESSIM: A simulator for the Athena-X-IFU

J. Wilms[a], S.J. Smith[b], P. Peille[c], M.T. Ceballos[d], B. Cobo[d], T. Dauser[a], T. Brand[a], R.H. den Hartog[e], S.R. Bandler[b], J. de Plaa[e], and J.-W.A. den Herder[e]

[a]Dr. Remeis-Sternwarte and Erlangen Centre for Astroparticle Physics, Universität Erlangen-Nürnberg, Sternwartstr. 7, 96049 Bamberg, Germany
[b]NASA Goddard Space Flight Center, Mail Code: 662, Greenbelt, MD 20771, USA
[c]Institut de Recherche en Astrophysique et Planétologie, 9 avenue du Colonel Roche, BP 44346, 31028 Toulouse Cedex 4, France
[d]Instituto de Fsica de Cantabria (CSIC-UC), Avda. de los Castros s/n, 39005 Santander, Spain
[e]SRON Netherlands Institute for Space Research, Sorbonnelaan 2, 3584 CA Utrecht, Netherlands

ABSTRACT

We present the design of `tessim`, a simulator for the physics of transition edge sensors developed in the framework of the *Athena* end to end simulation effort. Designed to represent the general behavior of transition edge sensors and to provide input for engineering and science studies for *Athena*, `tessim` implements a numerical solution of the linearized equations describing these devices. The simulation includes a model for the relevant noise sources and several implementations of possible trigger algorithms. Input and output of the software are standard FITS-files which can be visualized and processed using standard X-ray astronomical tool packages. `Tessim` is freely available as part of the SIXTE package (`http://www.sternwarte.uni-erlangen.de/research/sixte/`).

Keywords: Athena, simulation, transition edge detectors, X-ray detector

1. ATHENA END-TO-END-SIMULATIONS

The aim of ESA's *Athena* mission is the science of the Hot and Energetic Universe, especially the study of the emission from hot ($> 10^6$ K) plasmas, the search for missing baryons, and the study and evolution of the large scale structure and black holes. To meet these goals, *Athena* will have a single large-aperture (effective area $>15000\,\mathrm{cm}^2$ at 1 keV) X-ray telescope, based on silicon pore optics, and two focal plane instruments: The Wide Field Imager (WFI; [1]), a silicon-based DEPFET detector with a large field of view, high spatial resolution, and moderate energy resolution, and the X-ray Integral Field Unit (X-IFU; [2]), a cryogenic imaging spectrometer with a 5′ field of view, good spatial resolution, and very high energy resolution.

Part of the development strategy for both instruments is the parallel development of end-to-end simulation capabilities, in order to model the instrument performance and to be able to study how design decisions impact *Athena*'s science. This end-to-end simulation software is based on the SIXTE environment (`http://www.sternwarte.uni-erlangen.de/sixte`), a modular software environment released as open source. SIXTE was originally developed as the end-to-end simulation environment for the eROSITA instrument [3] on board *Spectrum-X-Gamma* [4, 5]. SIXTE consists of a large number of individual software modules, which are as much as possible written in an instrument independent way in order to maximize the reuse of existing software [6]. Astronomical sources are simulated using an advanced source model which allows to specify the properties of X-ray astronomical sources, including their spectral shape, spatial extent and variability properties. The source model scales well from single sources to whole sky simulations encompassing several 10^6 sources. Based on a Monte Carlo approach, in a simulation run photons are drawn from these sources and projected onto the focal plane where they are detected. The output of a SIXTE simulation are standard event files, i.e., photon lists, in

Further author information: (Send correspondence to J. Wilms
E-mail: joern.wilms@sternwarte.uni-erlangen.de

Space Telescopes and Instrumentation 2016: Ultraviolet to Gamma Ray, edited by Jan-Willem A. den Herder, Tadayuki Takahashi, Marshall Bautz, Proc. of SPIE Vol. 9905, 990564 · © 2016 SPIE · CCC code: 0277-786X/16/$18 · doi: 10.1117/12.2234435

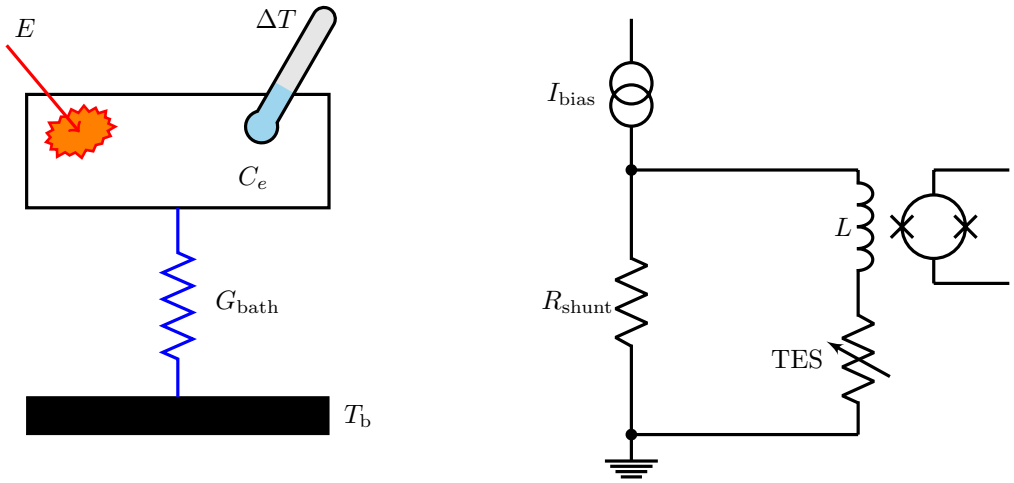

Figure 1. *Left:* Schematic picture of a TES (after [12]): A photon of energy E is absorbed in a material with heat capacity C_e, causing a temperature increase ΔT which causes a change in the resistance of the material. The material is coupled to a bath with temperature $T_{\rm b}$ with a thermal link with conductance $G_{\rm bath}$. *Right:* Electrical schematic of a TES system with bias current $I_{\rm bias}$, applied to a shunt resistor $R_{\rm shunt}$, an inductance L and the (variable resistance) TES. The system is read out with a SQUID (after Irwin & Hilton [13], Fig. 3).

the same FITS format that is also used for existing missions. This means that the processing of the simulated data can use already existing standard software packages such as HEASOFT, XSPEC [7], or ISIS [8, 9, 10].

The modular approach of SIXTE allows us to describe a given X-ray detector such as the X-IFU in different levels of detail. While the simulation of a faint, extended source might be addressed in sufficient detail with a simplified detector model that is based on the sensor's quantum efficiency and energy redistribution matrix, in other studies simulations of the read out process or energy reconstruction mechanism might be required. In the SIXTE approach such simulations can be obtained by replacing one single program in the simulation chain. Instruments are thus described at varying degrees of precision, depending on the simulation needs.

In this contribution we describe `tessim`, a simulator aiming at describing the microphysics of Transition Edge Sensors (TES) such as those employed within the X-IFU instrument. In Section 2 we describe the physical principle of Transition Edge Sensors and how the device is described in SIXTE. Section 3 describes some of the trigger algorithms used. Please see the accompanying contribution by Peille et al. [11] for a description of possible energy reconstruction algorithms. We give an outlook on the next steps of the development in Section 4.

2. SIMULATION APPROACH

Figure 1 illustrates the operating principle of a X-ray sensitive transition edge sensor [14], see Irwin and Hilton [13] for a review: A TES consists of an X-ray absorber with heat capacity C_e kept at its transition temperature to the superconducting regime ($\sim$90 mK). The absorber is coupled to a thermal bath ($T_{\rm bath} \sim 50$ mK). As a photon is absorbed in the detector, its energy E is deposited in the absorber. This leads to a time-dependent change in temperature, ΔT, from which the originally photon energy can be reconstructed (see Peille et al. [11], these proceedings, for an overview of the reconstruction methods).

`Tessim` is an improved and extended version of a TES simulation code originally developed at NASA-GSFC by Stephen J. Smith. The code is distributed as part of the SIXTE package and works on the Linux and MacOS operating systems as a command line tool. Input to `tessim` is a FITS file which contains the photon arrival times and energies, the output is a FITS file which contains the time dependent temperature and current at the desired sampling frequency. `tessim` also implements several typical triggering algorithms. In this case the output of `tessim` is a FITS file which only contains the triggered events (see below).

Table 1. Input parameters of `tessim`. In addition, the program has parameters describing the input photon event list, the output file type, the trigger algorithm, the seed of the random number generator, and whether the TES is AC or DC biased.

Parameter	Symbol	Typical Value	Explanation
Parameters describing the initial conditions			
`sample_rate`		156250	Sample rate [Hz]
`T_start`	$T_{\rm start}$	90.0	Initial operating temperature [mK]
`I0`	I_0	72.5	Initial current [μA]
Parameters describing TES properties			
`Ce`	$C_{\rm e}$	0.26	Heat capacity [pJ/K]
`Gb`	$G_{\rm bath}$	300	Bath conductance [pW/K]
`n`	n	4.0	Temperature exponent
`alpha`	α	100	TES sensitivity α
`beta`	β	10	TES current dependence β
`m_excess`	m	0.8	Magnitude of unexplained (excess) noise
`R0`	R_0	1.1	Operating point resistance [mΩ]
`Tb`	$T_{\rm bath}$	55	Heat sink/bath temperature [mK]
`RL`	$R_{\rm L}$	0.0	Shunt/load resistor value [mΩ]
`Rparasitic`	$R_{\rm parasitic}$	0.0	Parasitic resistor value [mΩ] (AC bias only)
`TTR`		4.11	Transformer Turns Ratio (AC bias only)
`Lin`	$L_{\rm in}$	238	Circuit inductance [nH] (DC only)
`Lfilter`	$L_{\rm filter}$	2	Filter inductance [μH] (AC only)
`V0`	V_0	I_0R_0	Effective voltage bias [μV]
Parameters describing the digital signal			
`imin`		-10^{-8}	TES current corresponding to 0 ADU [A]
`imax`		5×10^{-5}	TES current corresponding to 65534 ADU [A]
`adcbit`		16	Number of bits for the digitization

In order to model the TES, `tessim` performs a numerical solution of the differential equations for the time-dependent temperature, $T(t)$, and current, $I(t)$, in the TES [13],

$$C\frac{dT}{dt} = -P_{\rm b} + R(T,I)I^2 + P + \text{Noise} \tag{1}$$

$$L\frac{dI}{dt} = V - IR_{\rm L} - IR(T,I) + \text{Noise} \tag{2}$$

resulting in a realistic non-linear detector response with energy and non-stationary detector noise during an X-ray event. The transition edge is described by a linear resistance model,

$$R(T,I) = R_0 + \left.\frac{\partial R}{\partial T}\right|_{I_0}(T-T_0) + \left.\frac{\partial R}{\partial I}\right|_{T_0}(I-I_0) \tag{3}$$

where the partial derivatives are described with the parameters

$$\alpha = \left.\frac{\partial \log R}{\partial \log T}\right|_{I_0} = \frac{T_0}{R_0}\left.\frac{\partial R}{\partial T}\right|_{I_0} \tag{4}$$

$$\beta = \left.\frac{\partial \log R}{\partial \log I}\right|_{T_0} = \frac{I_0}{R_0}\left.\frac{\partial R}{\partial I}\right|_{T_0} \tag{5}$$

and where R_0, I_0, and T_0 are the operating point resistance, current, and temperature.

The model includes the thermal link to the thermal bath, which is modeled using a power law approximation,

$$P_{\rm b}(T,T_{\rm bath}) = \frac{G_{\rm bath}}{nT^{n-1}}\left(T^n - T_{\rm bath}^n\right) \tag{6}$$

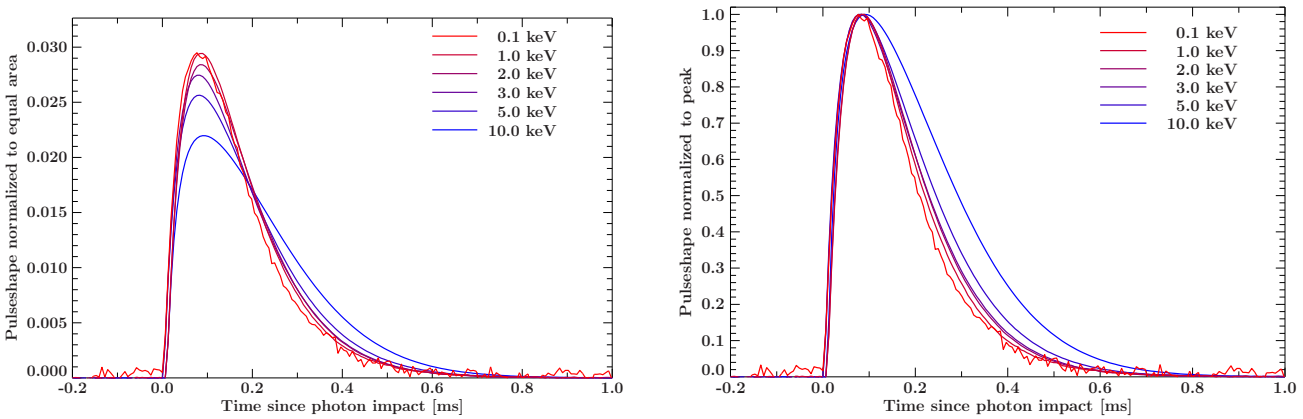

Figure 2. Variation of TES pulse shapes as a function of energy calculated with `tessim`, normalized to the same area (*left*) and maximum (*right*), respectively. Such simulations were used to define the X-IFU event grades and for the X-IFU focal plane optimization exercise (see [2]). In this and the following figures, currents are flipped and baseline subtracted.

where $G_{\rm bath}$ is the heat bath conductance and n is the temperature exponent. `tessim` can simulate both, AC biased and DC biased sensors.

The noise sources included in the model are thermal fluctuations between the TES and the heat bath, electrical Johnson noise of the TES and shunt resistor, and readout noise from the SQUID and amplifier chain. Also included is an unexplained noise parameter (based on empirical characterization) that represents sources of noise internal to the TES that are as yet not fully understood. These noise terms are modeled as Gaussian noise with the appropriate normalization, which takes into account the step size of the numerical integration. Table 1 gives a list of the input parameters of the simulation.

At the current time the numerical integration of Eqs. (1) and (2) is performed using a standard 4th order Runge-Kutta integrator taken from the Gnu Scientific Library (`https://www.gnu.org/software/gsl/`). We note that such integrators are not the best choice for stochastic differential equations, and are currently investigating different families of integrators better suited for such problems (e.g., [15, 16, 17]).

As an example, Fig. 2 shows the energy dependent, `tessim`-generated TES signals for one variant of the small pixel array currently discussed for the *Athena* X-IFU (see [2]). Note that the pulses are normalized to the same area and maximum current, respectively, in order to illustrate the variation of the pulse profile with energy. Figure 3 illustrates the variation of the overall pulse strength with photon energy.

3. TRIGGERING APPROACH

In addition to providing a full dump of $T(t)$ and $I(t)$ for the full simulation, `tessim` also implements a selection of trigger algorithms. In this case data records are written to file only if a trigger condition is met. Triggers operate on the digitized data signal, i.e., on a digitized version of the simulated current, $I(t_i)$, of the ith time step,

$$I_i = 2^{\texttt{adcbit}}\,\frac{I(t_i) - \texttt{imin}}{\texttt{imax} - \texttt{imin}} \tag{7}$$

where `adcbit` describes the number of bits of the digitization and where $\texttt{imin} \le I(t_i) < \texttt{imax}$. Values outside this range are flagged as errors.

Options to `tessim` allow both the generation of fixed length data records, as well as variable length records. For a given trigger, the output record has a length of `triggersize` samples, starting `prebuffer` samples before the trigger. Additional arguments to `tessim` allow to suppresses further triggers for `samples` time steps after the initial trigger. Setting $\texttt{samples} > \texttt{triggersize} - \texttt{prebuffer}$ prevents the creation of a further signal and thus produces a fixed length record which may or may not include the signal from more than one photon. Otherwise, if another trigger occurs while the program is already in triggered state, the output record length is adjusted to ensure that `triggersize` samples are also available for this second (or further) trigger.

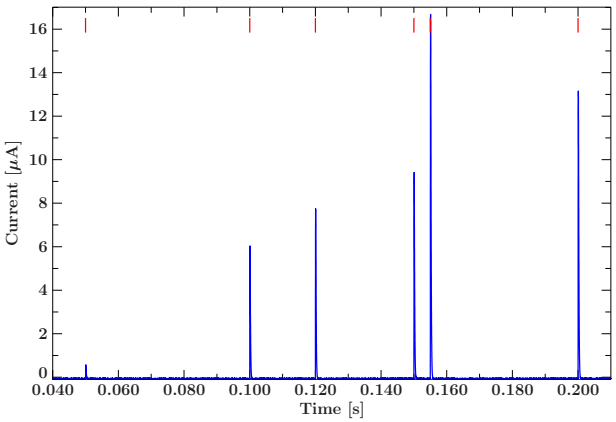

Figure 3. Example TES signal containing photon events with energies of 0.1, 1.0, 1.3, 1.6, 3.0, and 2.3 keV. The photon arrival times are indicated by the upper red tick-marks.

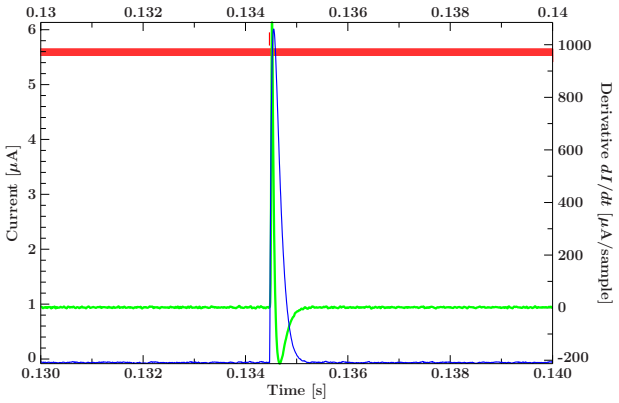

Figure 4. Example TES signal (blue) and its derivative (green). The red bar indicates the data record (in this case a stream), the theoretical photon arrival time is indicated by the upper red tickmarks, close to the maximum of the derivative.

The current version of tessim implements two trigger algorithms, further algorithms can easily be added:

1. Moving average: `movavg:npts:threshold:suppress`. The trigger condition is met if

$$\texttt{movavg}_i = \frac{1}{\texttt{npts}} \sum_{k=0}^{\texttt{npts}} I_{i-k-1} > \texttt{threshold} \tag{8}$$

2. Low-pass filtered differential trigger `diff:npts:threshold:suppress`. This algorithm triggers if the low pass filtered one-sided derivative of the signal,

$$I'_i = \sum_{k=0}^{\texttt{npts}} c_k I_{i-k} > \texttt{threshold} \tag{9}$$

where the coefficients c_k were derived by Pavel Holoborodko (`http://www.holobordko.com/pavel`). Our numerical experiments show that this family of low-noise differentiators appears to be more efficient than the more commonly used Savitzky-Golay [18]-Filters. Filters are implemented for $2 \leq \texttt{npts} \leq 10$. Figure 4 shows a simulated TES pulse and the left sided derivative obtained from the simulated signal.

4. OUTLOOK AND CONCLUSIONS

The current version of `tessim` has been used in initial studies of the X-IFU focal plane, including studies of the event grading [11], in deriving the bright source count rate constraints of the X-IFU, and in tradeoff studies for different pixel designs. As mentioned above, the code is freely available as part of the SIXTE package.

`tessim` is still under active development. The next steps to be added to the package are

1. Extension of `tessim` to multiple pixels, to allow full modeling of thermal and electronic cross talk,
2. Combination of `tessim` with the existing higher level X-IFU software, which already allows the simulation of the full focal plane of the detector (see Fig. 5),
3. Merging of `tessim` with the event reconstruction software SIRENA [11, 19, 20],
4. Better implementation of the nonlinearity of the transition edge, including saturation effects.

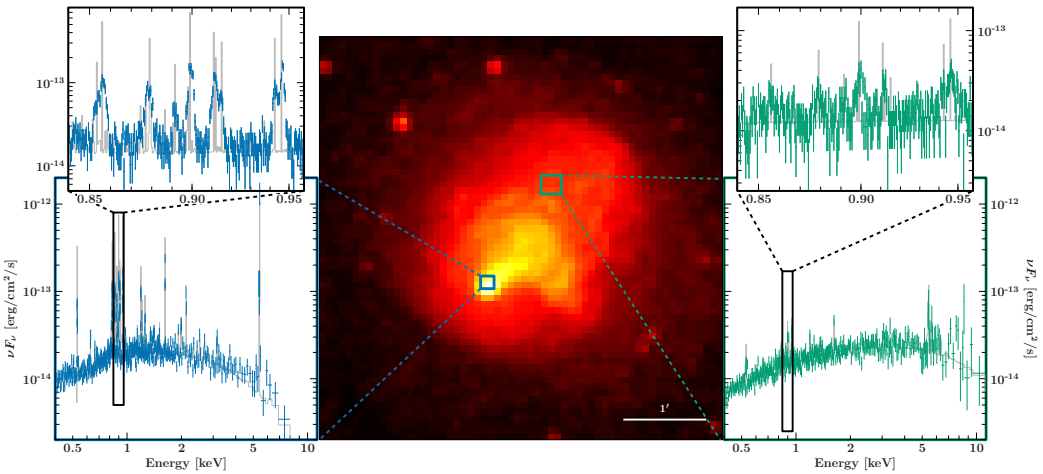

Figure 5. Simulation of TES spectra of the galaxy cluster Abell 2146 using the response matrix based simulator in SIXTE. The two plots show the spectra extracted from two small regions of the X-IFU image. Note the different strength and shape of the measured emission lines (colors), which indicate that X-IFU will be able to determine the temperature, density, turbulence, and bulk motion velocity at these locations. Grey lines show the underlying spectral model.

ACKNOWLEDGMENTS

This work made use of ISIS functions (`ISISscripts`) provided by ECAP/Remeis observatory and MIT (`http://www.sternwarte.uni-erlangen.de/isis/`). We thank J.E. Davis for the development of the `SLXfig` module, which was used to create all figures in this paper. JW, TB, and TD acknowledge funding by the Deutsches Zentrum für Luft- und Raumfahrt contract 50 QR 1402. MTC and BC acknowledge financial support by MINECO through grant ESP2014-53672-C3-1-P.

References

[1] Meidinger, N., Nandra, K., Plattner, M., Porro, M., Rau, A., Santangelo, A., Tenzer, C., and Wilms, J., "The Wide Field Imager Instrument for Athena," in [*Space Telescopes and Instrumentation 2014: Ultraviolet to Gamma Ray*], den Herder, J.-W. A. and Bautz, M., eds., *Proc. SPIE* **9144** (2014).

[2] Barret, D., den Herder, J.-W. A., Piro, L., Trong, T. L., Barcons, X., et al., "The Athena X-ray Integral Field Unit," in [*Space Telescopes and Instrumentation 2016: Ultraviolet to Gamma Ray*], *Proc. SPIE* **9905** (2016). These proceedings.

[3] Predehl, P., "eROSITA," in [*Space Telescopes and Instrumentation 2012: Ultraviolet to Gamma Ray*], *Proc. SPIE* **8443** (Sept. 2012).

[4] Kreykenbohm, I., Schmid, C., Wilms, J., Brunner, H., and Lamer, G., "eROSITA Near Real Time Analysis," in [*Astronomical Data Analysis Software and Systems XVIII*], Bohlender, D. A., Durand, D., and Dowler, P., eds., *Astron. Soc. Pacific, Conf. Ser.*(411), 285 (2009).

[5] Schmid, C., Martin, M., Wilms, J., Kreykenbohm, I., Mühlegger, M., Brunner, H., Fürmetz, M., Predehl, P., Kendziorra, E., and Barret, D., "Simulations of X-Ray Telescopes for eROSITA and IXO," in [*X-ray Astronomy 2009*], Comastri, A., Angelini, L., and Cappi, M., eds., *Am. Inst. Phys., Conf. Ser.*, 591–592 (July 2010).

[6] Wilms, J., Brand, T., Barret, D., den Herder, J.-W., Kreykenbohm, I., Lotti, S., Meidinger, N., Nandra, K., Peille, P., Piro, L., Rau, A., Schmid, C., Smith, R. K., Tenzer, C., Wille, M., and Willingale, R., "Athena end to end simulations," in [*Space Telescopes and Instrumentation 2014: Ultraviolet to Gamma-Ray*], Takahashi, T., den Herder, J.-W., and Bautz, M., eds., *Proc. SPIE* **9144** (2014).

[7] Arnaud, K. A., "XSPEC: The First Ten Years," in [*Astronomical Data Analysis Software and Systems V*], G. H. Jacoby & J. Barnes, ed., *Astronomical Society of the Pacific Conference Series* **101**, 17 (1996).

[8] Houck, J. C. and Denicola, L. A., "ISIS: An Interactive Spectral Interpretation System for High Resolution X-Ray Spectroscopy," in [*Astronomical Data Analysis Software and Systems IX*], Manset, N., Veillet, C., and Crabtree, D., eds., *Astron. Soc. Pacific, Conf. Ser.* **216**, 591 (2000).

[9] Houck, J. C., "ISIS: The Interactive Spectral Interpretation System," in [*High Resolution X-ray Spectroscopy with XMM-Newton and Chandra*], G. Branduardi-Raymont, ed. (Dec. 2002).

[10] Kühnel, M., Müller, S., Kreykenbohm, I., Schwarm, F.-W., Grossberger, C., Dauser, T., Nowak, M. A., Pottschmidt, K., Ferrigno, C., Rothschild, R. E., Klochkov, D., Staubert, R., and Wilms, J., "Simultaneous fits in ISIS on the example of GRO J1008−57," *Acta Polytechnica* **55**(2), 123–127 (2015).

[11] Peille, P., Ceballos, M. T., Cobo, B., Wilms, J., Bandler, S., Smith, S. J., Dauser, T., Brand, T., de Plaa, J., Barret, D., den Herder, J.-W., Piro, L., Barcons, X., and Pointecouteau, E., "Performance assessment of different pulse reconstruction algorithms for the Athena X-ray Integral Field Unit ," in [*Space Telescopes and Instrumentation 2016: Ultraviolet to Gamma Ray*], *Proc. SPIE* **9905** (2016). These proceedings.

[12] Smith, S. J., *Development of Transition Edge Sensor Distributed Read-Out Imaging Devices for Applications in X-ray Astronomy*, PhD Thesis, University of Leicester, Leicester (2006).

[13] Irwin, K. D. and Hilton, G. C., "Transition-edge sensors," in [*Cryogenic Particle Detection*], Enss, C., ed., 63–149, Springer, Berlin, Heidelberg (2005).

[14] Moseley, S. H., Mather, J. C., and McCammon, D., "Thermal detectors as x-ray spectrometers," *J. Appl. Phys.* **56**, 1257 (1984).

[15] Hernandez, D. B. and Spigler, R., "*A*-stability of Runge-Kutta methods for systems with additive noise," *BIT* **32**, 620–633 (1991).

[16] Tocino, A. and Ardanuy, R., "Runge-Kutta methods for numerical solution of stochastic differential equations," *J. Comp. Appl. Math.* **138**, 219–241 (2002).

[17] Rößler, A., "Runge-Kutta methods for the strong approximation of solutions of stochastic differential equations," *SIAM J. Numer. Anal.* **48**(3), 922–952 (2010).

[18] Savitzky, A. and Golay, M. J. E., "Smoothing and differentiation of data by simplified least suares procedures," *Anal. Chem.* **36**(8), 1627–1639 (1964).

[19] Ceballos, M. T., Cobo, B., Peille, P., Wilms, J., Brand, T., Dauser, T., Bandler, S., and Smith, S., "Athena X-IFU event reconstruction software: SIRENA," in [*Exploring the Hot and Energetic Universe: The first scientific conference dedicated to the Athena X-ray observatory*], Ehle, M., ed. (2015). available online at `http://www.cosmos.esa.int/web/conferences-archive/athena-2015`.

[20] Ceballos, M. T., Cobo, B., Peille, P., Wilms, J., Brand, T., Dauser, T., Bandler, S., and Smith, S., "SIRENA: a software package for the energy reconstruction of the Athena X-IFU events," in [*Astronomical Data Analysis Software an Systems XXV*], Lorente, N. P. F. and Shortridge, K., eds., *Astron. Soc. Pacific, Conf. Ser.*, Astron. Soc. Pacific, San Francisco (2016).